RSC Advances

PAPER

View Article Online
View Journal | View Issue

Cite this: *RSC Adv.*, 2024, **14**, 22403

Shape-controlled synthesis of micro-/nanosized Cu particles with spherical and polyhedral shapes using the polyol process†

Nguyen Thi Nhat Hang, [a] Yong Yang, [b] Le Hong Phuc,[c] Nguyen Huu Tri, [d] Ho Van Cuu[d] and Nguyen Viet Long *[d]

Received 17th May 2024
Accepted 28th June 2024

DOI: 10.1039/d4ra03643c

rsc.li/rsc-advances

This study reports the synthesis of Cu micro-/nanosized particles through the polyol process. Cu particles were synthesized by reducing copper(II) chloride in ethylene glycol (EG), polyvinylpyrrolidone (PVP), and potassium bromide (KBr) at low temperatures with or without the use of sodium borohydride ($NaBH_4$).

Introduction

In recent years, Cu-based metals, alloys, oxides and compounds with micro-/nanosized structures for catalysis, such as Cu, PtCu, CuO, Cu_2O, CuS, and $CuFe_2O_4$, have been reported.[1,2] Polyol processes have great advantages for synthesis using glycols, typically ethylene glycol (EG). However, the key issues of size, shape and composition limit their potential applications.[2] Cu nanoparticles are also synthesized *via* chemical methods.[3] In this view, the synthesis of Au and Ag nanocrystals with cubic and spherical shapes *via* polyol processes is of very special concern.[4] It is certain that the role of Br ions has led to the formation of cubic shapes of Ag nanoparticles.[5] Here, Cu nanograins show CO_2 electroreduction.[6] There are many works involved in the synthesis of Cu nanoparticles.[7–10] In an interesting work, Cu nanocubes were synthesized through a one-pot solution process using EG as a good solvent.[11] Additionally, Cu electrocatalysts of interest can convert CO_2 into C_{2+} products.[12,13] Cu and Cu@Cu–Ni nanocubes and nanowires were prepared in hydrophobic solution in the presence of Ni and Cl ions,[14] the controlled Cu nanocubes and Cu nano-octahedra,[7,15] cubic Cu catalysts,[8,9] and Cu nanocubes,[10] as well as the formation of large Cu oxide cubes.[16–18] The cubic shapes of Cu or CuPd obtained through the polyol processes were needed for CO_2 reduction.[19–22] The tailored Pt–Cu nanoparticles were used for the electrocatalysis of hydrogen evolution reactions.[23,24] The new roles of cubic and spherical shapes were significantly addressed in the synthesis and self-organization of Cu particles.[25–28] In another research study, Cu nanocrystals with high crystallization and stability were also formed in an aqueous solution with glucose as a reducing agent and hexadecylamine as a capping agent.[27] Additionally, researchers also focused on the high porosity of Cu particles.[28,29]

In this research study, we made our best efforts to synthesize Cu particles in the ranges of nm and μm. The cubic and spherical shapes were controlled and obtained through the polyol processes.

Materials and methods

In our research, we used 10 mL EG, 1 mL of the k ratio of $CuCl_2$ (0.0625 M), 2 mL of PVP (0.375 M) ($k = [PVP]/[Cu^{2+}]$; $k = 6$), and 2 mL $NaBH_4$ (0.0625 M) for the synthesis of Cu particles in the nanometer range (Sample 1). The mixture was stirred at 160 °C for 3 h in a three-neck flask. We used 10 mL EG, 5 mL of the k ratio of PVP and $CuCl_2$ ($k = [PVP]/[Cu^{2+}]$; $k = 2$), and 1.5 mL NaOH 0.02 M for the synthesis of Cu particles in the nano-/micrometer range (Sample 2). The mixture was stirred at 150 °C for 3 h in a three-neck flask. We used 10 mL EG, 5 mL of the k ratio of $CuCl_2$ and PVP ($k = [PVP]/[Cu^{2+}]$; $k = 2$), 1.5 mL NaOH (0.02 M), and 0.5 mL KBr (2 mM) (Sample 3). The mixture was stirred at 150 °C for 3 h in the three-neck flask. We used UV-vis (Lamda spectrometer, 950 Model; EMC-NANO-UV Spectrophotometer), XRD (Rigaku D/max 2550V; Panalytical X'PERT PRO, The Netherlands), SEM (S-4800), and TEM measurements (JEM-2100F) for the characterization of the as-prepared micro/nanosized Cu nanoparticles by the polyol process.

Results and discussion

Fig. 1 shows that the size of the as-prepared Cu nanoparticles was confirmed in the nanosized range, especially for most Cu

[a]*Institute of Applied Technology, Thu Dau Mot University, 6 Tran Van On, Phu Hoa Ward, Thu Dau Mot City 820000, Vietnam*

[b]*State Key Laboratory of High-Performance Ceramics and Superfine Microstructures, Shanghai Institute of Ceramics, Chinese Academy of Sciences, 1295 Dingxi Road, Shanghai, 200050, China*

[c]*National Institute of Applied Mechanics and Informatics, Vietnam Academy of Science and Technology, 291 Dien Bien Phu, Ho Chi Minh City 700000, Vietnam*

[d]*Department of Electronics and Telecommunications, Saigon University, 273 An Duong Vuong, District 5, Ho Chi Minh City 700000, Vietnam. E-mail: nguyenvietlong@sgu.edu.vn*

† Electronic supplementary information (ESI) available. See DOI: https://doi.org/10.1039/d4ra03643c

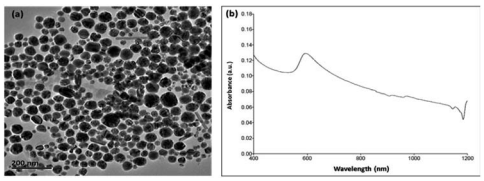

Fig. 1 (a) TEM image of nanosized Cu particles with a size less than 100 nm, (b) UV-vis measurement and (c) XRD. See more: ESI† (Sample 1).

nanoparticles with a size less than 100 nm and surface plasmonic band (SPR) at about 600 nm (Sample 1). Fig. 1 also shows the XRD results of the crystal structure of Cu nanoparticles of the face-centered cubic (fcc) lattice showing that the peaks at different angles characterize the structural aspects of Cu nanoparticles with high crystallization, corresponding to the fine crystal planes at (111), (200), (220), and (311). The crystal parameters of Cu nanoparticles were found in good accordance with the pattern of Cu (PDF#04-0836) with the intensity of the strongest (111) crystal plane. In this process, $CuCl_2$ (for the formation of Cu particles) and EG (both solvent and weak reducing agent) were used with PVP (protective agent) and $NaBH_4$ (modifying or strong reducing agent). The formation of Cu nanoparticles was determined by a typical equation ($2Cu^{2+} + BH_4^- + 2H_2O + 2n\text{PVP} \rightarrow 2Cu(PVP)_n + 2H_2 + 4H^+ + BO_2^-$). Fig. 2, *i.e.* XRD and UV data, shows the same result of XRD as Fig. 1 (see more ESI†) but a very different result of SPR. The band of SPR (Fig. 2b) was largely extended in comparison with that of SPR (Fig. 1b). The XRD data of (*hkl*) of Fig. 1a was relatively similar to Fig. 2a in the standard pattern of Cu (PDF#04-0836 or 85-1326).

The collective vibrations of charge clouds (the negative and positive charge clouds of the surfaces of the very small estimated spherical Cu particles in the micro/nanosized range are very different from those of the estimated large cubic and spherical Cu particles in the micro/nanosized range). It is certain that the addition of NaOH also resulted in a very good reduction of $CuCl_2$ salt in the EG solvent. XRD data analysis demonstrated that Cu particles are produced during this reduction process. It is obvious that the obtained UV-vis spectrum shows the 600 nm peak of Cu nanoparticles (Fig. 1a), however, the plasmon band is much wider due to the size of the particle being too large with cubic and spherical shapes, or rectangular-type shapes or polyhedral shapes of large Cu particles (Fig. 2b). On the other hand, an additional peak of 500 nm appears, most of the produced particles may be of spherical shapes but have many absorption surfaces.

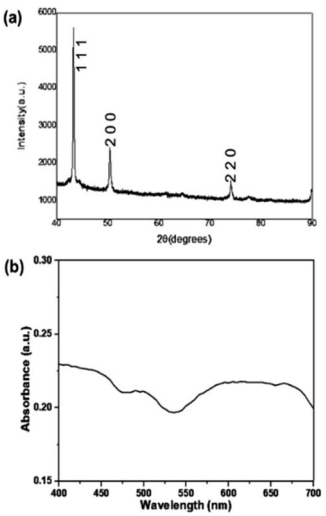

Fig. 2 (a) XRD spectrum of the micro-/nanosized Cu particles (Sample 2) and (b) UV-vis measurement. See more: ESI.†

A small amount of KBr was added (K^+, Br^- ions) that lead to the formation of Cu particles in the form of cubes (assembly), spheres (assembly), and large clusters of the assembled nanoparticles by SEM (S-4800).

Here, it is known that collisions between two particles, multiple particles, and their combinations are the most common phenomena that create new, larger particles. There is a new phenomenon where the collision of metal particles (nano or micro size) creates a new particle according to the soft collision mechanism from two particles or a formation of a new large cluster from many very small particles. The final shape and size were proposed according to the mechanism of keeping the shape of the two particles stuck together or creating a new type of particle after recrystallization as shown in Fig. 3. We also understand that the collision processes of the two particles or many particles need to be investigated in the detail. The common collision processes of nano/microparticles can be clearly observed in their SEM images. Because of the fast movement between them, specific interactions between two particles occur. The strongest interactions between the particles can be seen in Fig. 3 because of the fast movement and very large interaction forces between them. This is not self-assembly of the nanoparticles. Thus, the strong interactions of the particles due to the motion may be elastic and inelastic collisions. In the case of inelastic collisions, the particles can be randomly combined. This leads to the formation of new bigger particles if they are inelastic collisions. The particles can be cracked and broken into smaller particles if there are partly inelastic collisions. The forms of elastic and inelastic collisions of large particles can also lead to the formation of small pieces or smaller particles (Fig. 4 and 5). The deformations of surfaces of particles can be observed in our evidence of SEM images of large particles in the μm range. In the controlled synthesis of metal and oxide-based particles or nanoparticles, collision phenomena were significantly ignored. However, we think that collision phenomena are very important during the first stages of nucleation, growth, and the formation of very tiny nanoparticles. From our results and data, we also predict that collision phenomena are very crucial to controlling the size and the shape of the prepared particles by chemical and physical methods. The most interesting phenomena of nucleation, collision, attachment, growth, and formation can occur very quickly, which are the main causes of the formation of nano or microsystems under suitable experimental conditions and control processes according to the experiences of researchers.

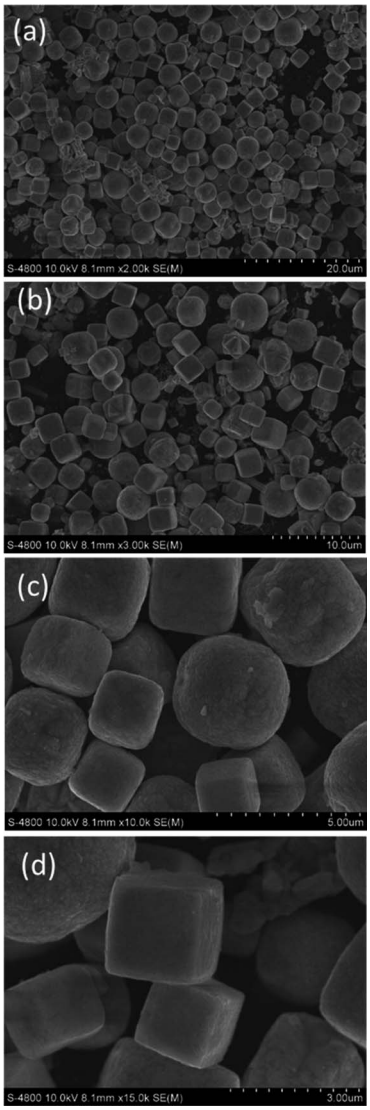

Fig. 3 SEM image of the micro-/nanosized Cu particles. Scale bars: (a) 20 μm (Sample 2). (b) 10 μm (Sample 3). (c) 5 μm and (d) 3 μm (Sample 2). The size and shape are appropriately evaluated. See more: ESI.†

In the ethanol solution, most large particles formed have their various velocities during mixing by an ultra-sonication source for several minutes or more time, even by heat sources. The high stability and durability of particles were proven in our experiment. Therefore, the various elastic and inelastic collisions can occur in various directions by mixing and heating. As a result, we can see the large clusters of particles after collisions. Most of the large particles could also retain size, shape, and morphology after all the experimental processes, such as synthesis and centrifugation. They can be influenced by collision and heat processes in solutions or the environment of measurements, *i.e.* SEM. The deep knowledge of collision mechanisms, growth, and formation of many large nanoparticles between two particles, three particles, and a large amount of many particles in a system has been not

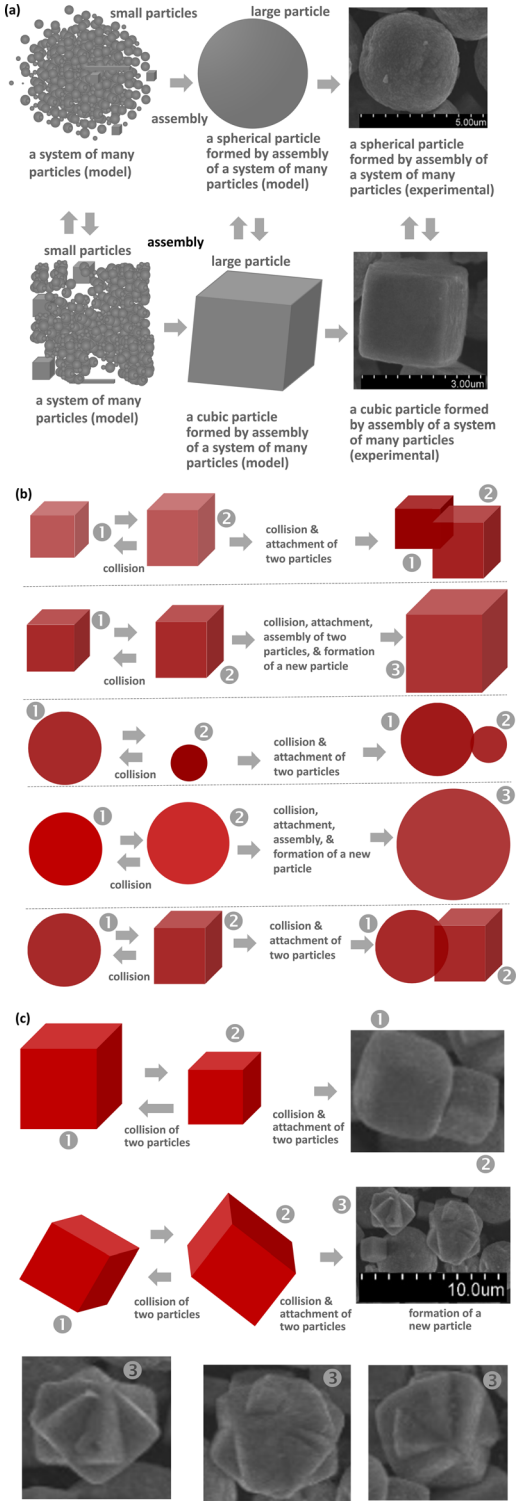

Fig. 4 Models: (a) formation of various spherical and cubic particles by assembly. (b) Attachment. (c) Collision, attachment, and formation of two cubic particles of a new large particle according to experimental evidence in the colloidal synthesis. (1) and (2) Labels are for the as-prepared particles with cubic and spherical shape, respectively. (3) A new particle (about 3–4 μm). See more: ESI.†

transparently understood in comparison with the case of the above collisions between two particles (Fig. 4 and 5).

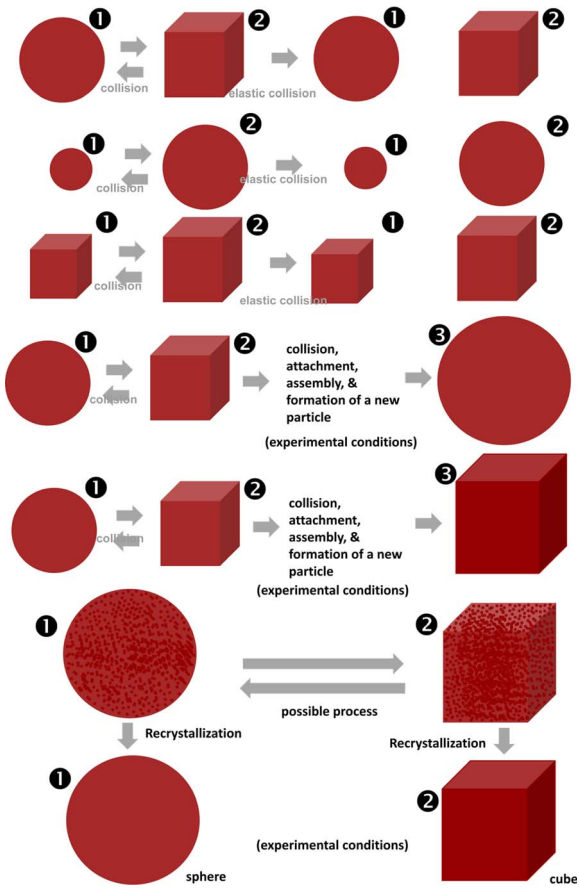

Fig. 5 A model for the formation of large spherical and cubic particles by assembly (Labels: (1) spherical particle; (2) cubic particle; and (3) a formation of a new particle with spherical or cubic shape). See more: ESI.†

The interesting elastic recoveries of the particles of structures, shapes, and morphologies are very good after collisions due to the elastic and inelastic phenomena (Fig. 5). It is suggested that large particles were formed by various collisions with or without self-assembly. In a work of crystal structure and composition, the pure crystal structures of the as-prepared Cu nanoparticles have shown peaks at about 932.7 and 952.5 eV by XPS corresponding to $Cu2p_{3/2}$ and $Cu2p_{1/2}$, respectively.[30] Researchers have also used anion exchange reactions or polyol-based reactions for the formation of Cu_2O and CuS in the controlled synthesis.[31,32]

Conclusions

In this research, we confirm that the motion mechanism and collision of the as-prepared nanoparticles in the environment, *i.e.* solution, solvent, air, and gas are clearly considered important factors, leading to the collision processes such as elastic and/or inelastic collisions under strong mixing conditions allowing the final formation of large crystals. In special cases, most collisions between nanoparticles need to be effectively controlled in the elastic forms in certain experimental conditions for controlled nano, micro, or micro-nanosystems. These are the main causes why the same process can lead to different results producing nanoparticles of various sizes and shapes in a small change of experimental steps, such as time, mixing rate, temperature, and other related factors. The polyol processes for the synthesis of micro/nanosized materials can meet the demands and challenges that remain to possibly control the defined sizes of particles in the defined ranges of nm and μm, their shapes in the sharp polyhedral or spherical forms, their micro/nanosized structures, and their compositions in synthesis and preparation processes.

Data availability

The data presented in our research do not involve animal or human health data.

Author contributions

N. V. L. conducted the experiments, collected the data and results, wrote the entire original manuscript, and discussed the results and insights into the polyol processes for the synthesis of Cu nanoparticles. N. V. L., Y. Y., L. H. P., N. H. T., N. T. N. H., and H. V. C. discussed experimental data and research results.

Conflicts of interest

There are no conflicts to declare.

Acknowledgements

Our research was supported by Saigon University through Grant number CSA2022-20. This research is funded by Vietnam National Foundation for Science and Technology Development (NAFOSTED) under grant number 103.02-2021.32.

References

1 M. B. Gawande, A. Goswami, F. X. Felpin, T. Asefa, X. Huang, R. Silva, X. Zou, R. Zboril and R. S. Varma, *Chem. Rev.*, 2016, **116**, 3722.
2 (*a*) F. Fiévet, S. Ammar-Merah, R. Brayner, F. Chau, M. Giraud, F. Mammeri, J. Peron, J. Y. Piquemal, L. Sicard and G. Viau, *Chem. Soc. Rev.*, 2018, **47**, 5187; (*b*) S. Ammar and F. Fiévet, *Nanomater.*, 2020, **10**, 1217.
3 N. A. Dhas, C. Paul Raj and A. Gedanken, *Chem. Mater.*, 1998, **10**, 1446.
4 Y. Sun and Y. Xia, *Science*, 2002, **298**, 2176.
5 F. Wu, W. Wang, Z. Xu and F. Li, *Sci. Rep.*, 2015, **5**, 10772.
6 Y. Yang, S. Louisia, S. Yu, J. Jin, I. Roh, C. Chen, M. V. F. Guzman, J. Feijóo, P. C. Chen, H. Wang and C. J. Pollock, *Nature*, 2023, **614**, 262.
7 S. C. Lu, M. C. Hsiao, M. Yorulmaz, L. Y. Wang, P. Y. Yang, S. Link, W. S. Chang and H. Y. Tuan, *Chem. Mater.*, 2015, **27**, 8185.
8 P. Grosse, A. Yoon, C. Rettenmaier, A. Herzog, S. W. Chee and B. R. Cuenya, *Nat. Commun.*, 2021, **12**, 6736.

9 C. G. Morales-Guio, E. R. Cave, S. A. Nitopi, J. T. Feaster, L. Wang, K. P. Kuhl, A. Jackson, N. C. Johnson, D. N. Abram, T. Hatsukade and C. Hahn, *Nat. Catal.*, 2018, **1**, 764.
10 S. Thoka, M. Madasu, C. F. Hsia, S. Y. Liu and M. H. Huang, *Chem.–Asian J.*, 2017, **12**, 2318.
11 Y. Wang, P. Chen and M. Liu, *Nanotechnology*, 2006, **17**, 6000.
12 T. Kim and G. T. R. Palmore, *Nat. Commun.*, 2020, **11**, 3622.
13 A. Loiudice, P. Lobaccaro, E. A. Kamali, T. Thao, B. H. Huang, J. W. Ager and R. Buonsanti, *Angew. Chem., Int. Ed.*, 2016, **55**, 5789.
14 H. Guo, Y. Chen, H. Ping, J. Jin and D. L. Peng, *Nanoscale*, 2013, **5**, 2394.
15 S. Thoka, M. Madasu, C. F. Hsia, S. Y. Liu and M. H. Huang, *Chem.–Asian J.*, 2017, **12**, 2318.
16 X. Wang, C. Liu, B. Zheng, Y. Jiang, L. Zhang, Z. Xie and L. Zheng, *J. Mater. Chem. A*, 2013, **1**, 282.
17 Y. Bai, T. Yang, Q. Gu, G. Cheng and R. Zheng, *Powder Technol.*, 2012, **227**, 35.
18 Q. Hua, T. Cao, X. K. Gu, J. Lu, Z. Jiang, X. Pan, L. Luo, W. X. Li and W. Huang, *Angew. Chem.*, 2014, **126**, 4956.
19 F. Fievet, F. Fievet-Vincent, J. P. Lagier, B. Dumont and M. Figlarz, *J. Mater. Chem.*, 1993, **3**, 627.
20 G. Zhou, M. Lu and Z. Yang, *Langmuir*, 2006, **22**, 5900.
21 Z. Lyu, S. Zhu, L. Xu, Z. Chen, Y. Zhang, M. Xie, T. Li, S. Zhou, J. Liu, M. Chi and M. Shao, *J. Am. Chem. Soc.*, 2020, **143**, 149.
22 (*a*) N. V. Long, M. Ohtaki, T. D. Hien, J. Randy and M. Nogami, *Electrochim. Acta*, 2011, **56**, 9133; (*b*) N. V. Long, M. Ohtaki, M. Uchida, R. Jalem, H. Hirata, N. D. Chien and M. Nogami, *J. Colloid Interface Sci.*, 2011, **359**, 339; (*c*) N. V. Long, T. Asaka, T. Matsubara and M. Nogami, *Acta Mater.*, 2011, **59**, 2901; (*d*) N. V. Long, N. D. Chien, T. Hayakawa, H. Hirata, G. Lakshminarayana and M. Nogami, *Nanotechnology*, 2009, **21**, 035605; (*e*) N. V. Long, Y. Yang, T. Teranishi, C. M. Thi, Y. Cao and M. Nogami, *RSC Adv.*, 2015, **5**, 56560; (*f*) N. T. N. Hang, Y. Yang, N. Q. T. Nam, M. Nogami, L. H. Phuc and N. V. Long, *Crystals*, 2022, **12**, 375; (*g*) N. V. Long, N. T. N. Hang, Y. Yang and M. Nogami, Synthesis of Cobalt and Its Metallic Magnetic Nanoparticles, in *Handbook of Magnetic Hybrid Nanoalloys and Their Nanocomposites*, Springer, Cham, 2022; (*h*) N. V. Long, Y. Yang, T. Teranishi, C. M. Thi, Y. Cao and M. Nogami, *Mater. Des.*, 2015, **86**, 797; (*i*) N. V. Long, C. M. Thi, M. Nogami and M. Ohtaki, *New J. Chem.*, 2012, **36**, 1320.
23 D. Kaya, I. Demiroglu, I. B. Isik, H. H. Isik, S. K. Çetin, C. Sevik, A. Ekicibil and F. Karadag, *Int. J. Hydrogen Energy*, 2023, **48**, 37209.
24 M. A. B. Aissa, B. Tremblay, A. Andrieux-Ledier, E. Maisonhaute, N. Raouafia and A. Courty, *Nanoscale*, 2015, **7**, 3189.
25 H. J. Yang, S. Y. He, H. L. Chen and H. Y. Tuan, *Chem. Mater.*, 2014, **26**, 1785.
26 H. Guo, Y. Chen, M. B. Cortie, X. Liu, Q. Xie, X. Wang and D. L. Peng, *J. Phys. Chem. C*, 2014, **118**, 9801.
27 M. Jin, G. He, H. Zhang, J. Zeng, Z. Xie and Y. Xia, *Angew. Chem., Int. Ed.*, 2011, **50**, 10560.
28 (*a*) N. R. Jana, Z. L. Wang, T. K. Sau and T. Pal, *Mater. Sci.*, 2000, **79**, 1367; (*b*) R. Lu, W. Hao, L. Kong, K. Zhao, H. Bai and Z. Liu, *RSC Adv.*, 2023, **13**, 14361.
29 Z. Lyu, Y. Shang and Y. Xia, *Acc. Mater. Res.*, 2022, **3**, 1137.
30 M. Raja, J. Subha, F. B. Ali and S. H. Ryu, *Mater. Manuf. Processes*, 2008, **23**(8), 782.
31 H. L. Wu, R. Sato, A. Yamaguchi, M. Kimura, M. Haruta, H. Kurata and T. Teranishi, *Science*, 2016, **351**(6279), 1306.
32 Z. Li, M. Saruyama, T. Asaka, Y. Tatetsu and T. Teranishi, *Science*, 2021, **373**(6552), 332.